

# Modeling and performance calculation of a horizontal axis wind and hydrokinetic turbine: Numerical study

Anastas Yangyozov<sup>1</sup>, Damjanka Dimitrova<sup>1</sup>, and Lazar Panajotov<sup>2</sup>

1 – Technical University of Varna, Department of Thermal Engineering, 9010, 1 Studentska Street, Varna, Bulgaria

2 – Dobrudja College of Technology-Dobrich, Dobrotica 12, 9302, Dobrich, Bulgaria

Corresponding author contact: [yangyozovtu@tu-varna.bg](mailto:yangyozovtu@tu-varna.bg)

**Abstract.** A small turbine, working with air and water to generate electricity, was designed and its performance was reported in this paper. The rotor diameter is 150mm. The numerical calculations of the power coefficient, torque, and tip speed ratio of turbine were carried out for a wide range of inlet velocities. The flow passing through the turbine was investigated with commercial CFD code ANSYS CFX 18.

**Keywords:** Wind turbine, Hydrokinetic turbine, Numerical analysis, ANSYS CFX

## 1 Introduction

The number of hydrokinetic devices for the utilization of wind and water current energy has been increasing over the recent years. The elements of such devices can be manufactured relatively easily if using the 3D printing technology. Small-size portable devices have been designed to demonstrate their benefits. A clear example for that is the turbine of the company “Seaformatics“, which is adapted to work both in air and water. It should be kept in mind, that when we speak about renewable energy sources, serious attention should be paid on the production technology. The manufacturing technology should be waste-free or at least with reduced amount of waste. The elements of the turbine can be produced from recycled plastic waste. Hydrokinetic turbines can be combined with solar panels, fuel cells and other well-known in the practice equipment for the utilization of the energy from renewable sources.

This study shows the aerodynamic design of a horizontal-axis wind turbine blade operating with air and with water using CFD modeling with ANSYS CFX. This type of modeling is widely applied nowadays prior to manufacturing a new product. It allows studying the movement of a fluid through the turbine’s disk of impeller, as well as to assess the efficiency, weight, and last but not least, the price of the device. This work reports on the ongoing development of 3D CFD of a twist bladed horizontal axis wind and hydrokinetic turbine. Performance parameters including power and power coefficient were calculated.

The turbine, connected to a RIM generator, was patented in 1919 by the American engineer Harza (Miller H, 1974). This type of electrical machine has been used by “Sulzer Escher Wyss of Zurich“ in some 100 turbines by the name of “Straflo“ (Straight-flow turbine), where until 1984, the diameter of the impeller was up to  $D=3.7\text{m}$ . Nowadays, the RIM generator technology is applied in the practice, and the “Openhydro“ turbines are manufactured with a diameter of  $D=16\text{m}$  (Djebbari S, 2015) and rated power 500kW.

Fig.1, a and b shows one and the same turbine Waterlily (waterlilyturbine, 2018), (greenforwardnews, 2018), which first works in the air (a) and then in water (b). With one and the same speed of the inlet flow, the turbine generated power is different. This is due to the different densities of the air and of the water.

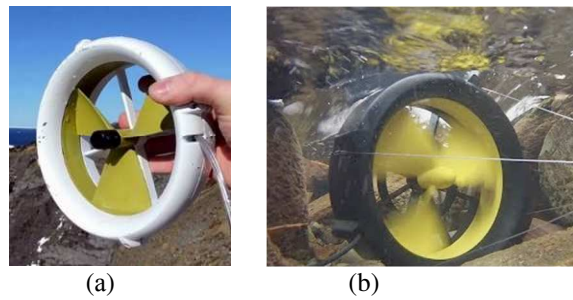


**Fig. 1.** Waterlily turbine working with air (a) and water (b)

Table 1 presents the main parameters of the Waterlily turbine when working with air, and when working with water. A turbine similar to that type is studied in the current paper. It is a suitable model, since there is available information about the power range that it can accomplish.

**Table 1.** Waterlily technical specifications (greenforwardnews, 2018), (waterlilyturbine, 2018).

|                                | Wind powered | Water powered |
|--------------------------------|--------------|---------------|
| Flow for power output 15W, m/s | 16.1         | 1.6           |
| Flow for power output 25W, m/s | 20.0         | 2.0           |
| Minimum fluid speed, m/s       | 3.0          | 0.3           |
| Maximum fluid speed, m/s       | 25.0         | 3.0           |

## 2 Modeling the turbine in the ANSYS Workbench environment

### 2.1 Numerical modeling and main parameters

A computer model is established before starting testing the real-life object in order to determine the main characteristics of the turbine, calculate the load of the elements, as well as evaluate the performance. The preliminary assessment of the weight of the whole installation allows for determining the price of the device, which is important for the client. The wide-spread commercial CFD codes of the CFX and Fluent modules are part of the ANSYS Workbench platform.

For studying the turbulent flow movement through the turbines flowing section are used the following numerical methods: Direct Numerical Simulation (DNS); Large Eddy Simulation (LES); Reynolds Average Navier-Stokes Equations (RANS) and Unsteady Reynolds Average Navier-Stokes Equations (URANS).

In this paper, CFD simulations are performed with the aim of ANSYS CFX 18.0. The last is wide spread nowadays commercial CFD code used by turbomachinery specialists all over the world. A numerical method is set in the software product ANSYS CFX – the finite volume method. Governing equations and turbulence model equations, which are discretizing, are:

$$\frac{\partial \rho}{\partial t} + \frac{\partial}{\partial x_j} (\rho U_j) = 0 \tag{1}$$

$$\frac{\partial}{\partial t} (\rho U_i) + \frac{\partial}{\partial x_j} (\rho U_j U_i) = -\frac{\partial P}{\partial x_i} + \frac{\partial}{\partial x_j} \left( \mu_{eff} \left( \frac{\partial U_i}{\partial x_j} + \frac{\partial U_j}{\partial x_i} \right) \right) \tag{2}$$

$$\frac{\partial}{\partial t} (\rho \phi) + \frac{\partial}{\partial x_j} (\rho U_j \phi) = \frac{\partial}{\partial x_j} \left[ \Gamma_{eff} \left( \frac{\partial \phi}{\partial x_j} \right) \right] + S_\phi \tag{3}$$

$$\frac{\partial (\rho k)}{\partial t} + \frac{\partial (\rho U_j k)}{\partial x_j} = P_k - \beta^* \rho k \omega + \frac{\partial}{\partial x_j} \left[ \left( \mu + \frac{\mu}{\sigma_{k3}} \right) \frac{\partial k}{\partial x_j} \right] \tag{4}$$

$$\frac{\partial (\rho \omega)}{\partial t} + \frac{\partial (\rho U_j \omega)}{\partial x_j} = \alpha_3 \frac{\omega}{k} P_k - \beta_3 \rho k \omega^2 + (1 - F_1) \frac{2\rho}{\sigma_{\omega 2} \omega} \frac{\partial k}{\partial x_j} \frac{\partial \omega}{\partial x_j} + \frac{\partial}{\partial x_j} \left[ \left( \mu + \frac{\mu}{\sigma_{\omega 3}} \right) \frac{\partial \omega}{\partial x_j} \right] \tag{5}$$

continuity (1) and momentum (2) equations in stationary and in moving subdomains, where  $U$  is the absolute velocity of fluid particle; eq.(3)-scalar  $\phi$  transport equation and in addition, the turbulence is modeled using a blended  $k-\omega/k-\varepsilon$  shear stress transport (SST) model, in which the turbulent kinetic energy  $k$  and specific dissipation rate  $\omega$  are modeled, which are described with SST turbulence model equations (4) and (5)- (ANSYS CFX-Solver, 2017), (Menter F, 2003).

With the analysis of the turbine, there are dependencies used, which are known from the theory of the wind and water turbines. They are presented below and are set as calculation dependencies in calculating power, power coefficient and the non-dimensional indicator TSR (Fleisinger M, 2014). The latter is defined as the ratio of the speed of the rotor tip to the free stream fluid velocity. The Tip Speed Ratio (TSR):

$$TSR = \frac{\omega \cdot R}{U_{\infty}} \quad (6)$$

is relationship between angular velocity  $\omega$  [rad/s], turbine radius at tip  $R$  [m] and  $U_{\infty}$  [m/s] is the current water or wind velocity.

The available power of the water/wind flow  $P_{avail}$  can be calculated using the following equation:

$$P_{avail} = \frac{1}{2} \cdot \rho \cdot A \cdot U_{\infty}^3 \quad (7)$$

where  $\rho$  is the water density and  $A$  is the cross-sectional area.

The power extracted from the fluid by the rotor of turbine  $P_{turb}$  is defined as:

$$P_{turb} = \omega \cdot T \quad (8)$$

where  $T$  is the torque on a turbine shaft.

The power coefficient  $C_p$  of a turbine can be calculated as:

$$C_p = \frac{P_{turb}}{P_{avail}} = \frac{\omega \cdot T}{\frac{1}{2} \cdot \rho \cdot A \cdot U_{\infty}^3} \quad (9)$$

Torque of blade is calculated using command which extracts data from CFD-Post. This data contains pressure values on blade surfaces which are projected normal to axis of rotation, in this case this is axis  $Z$ . The maximum value of the power coefficient is  $C_{p,max}=16/27$ . This is the theoretically maximum possible value and is also known in the specialized literature as Betz limit (Mannwell J, 2009).

## 2.2 Turbine description

Table 2 presents the main dimensions of the modeled turbine. The classic theories for profiling wind and water turbines are used in developing the turbine. Obtaining twisted blade is possible through 3D printing. The turbine consists of 3 blades rotating at  $TSR = 0.1 \div 0.8$ . The radius at hub is 10mm and at shroud is 75mm.

**Table 2.** Main dimensions of turbine

| Main dimensions         | Geometry                    |
|-------------------------|-----------------------------|
| Number of blades        | 3                           |
| Blade airfoil           | Variable from hub to shroud |
| Impeller diameter, mm   | 150                         |
| Impeller width, mm      | 30                          |
| Fluid domain length, mm | 300                         |

### 2.3 3D modeling of blades

There are blades in a cylindrical coordinate system created in BladeModeler module, and the shape of their leading edge-ellipse is modeled, as well as the shape of their trailing edge – circle.

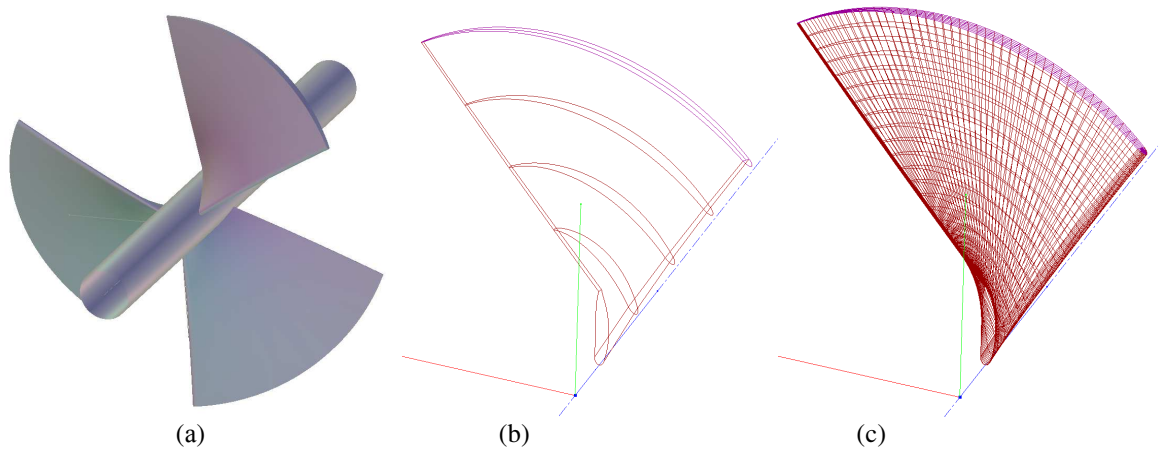


**Fig. 2.** 3D model procedure of turbine blade airfoils in BladeModeler

Besides, the law for the thickness distribution along camber line is changed. These operations are made for five layers (fig.2, b), defined by the user as follows -0% (hub), 25%, 50% (middle), 75% and 100% (shroud). The rotating domain around the turbine is 150 mm in diameter and 300 mm in length.

After modeling the 3-dimensional shape of the turbine blades, starts the transferring of the model from the specific turbo-module BladeModeler to DesignModeler. If there is a license to work with turbo modules in the DesignModeler environment, this transferring is carried out very easily with no complicated operations or typing of commands. The adding into the geometrical module is done in order to form the fluid domain, and then the solid domain of the blades is separated. The latter are not necessary since the present project studies only the fluid flow movement, while the stress analysis will be done at a later stage.

### 2.4 Mesh generation

The rotating domain is modelled in a structured manner with 393558 elements and 431043 nodes. The quality of the mesh elements is to be observed when forming the mesh around the twisted blade. There should not be any overstretched, too long or sharp elements.

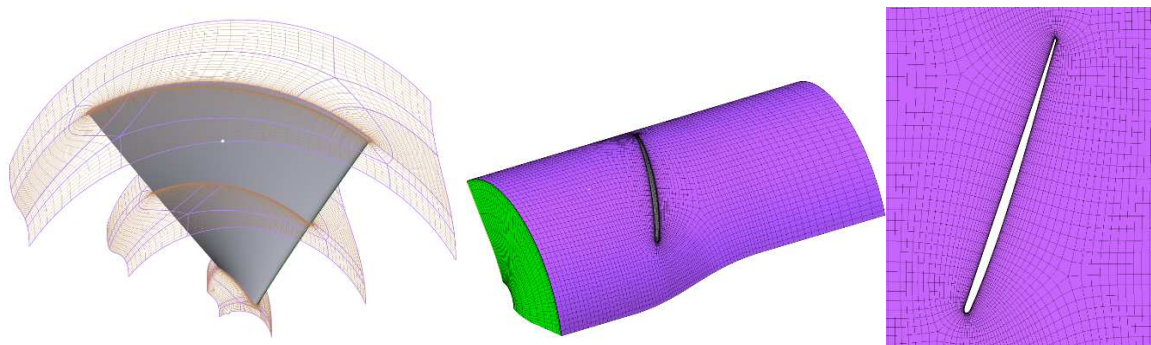


**Fig. 3.** Mesh generation procedure of fluid domain. Virtual topology definition (a), 3D mesh view (b) and blade-to-blade mesh view with O-grid around airfoil (c)

The elements' quality criteria are set out in the TurboGrid module. The presence of negative volumes should also be looked for. They must be definitely removed from the fluid domain. A special O-grid is generated around the blade, where the resolution of the mesh is controlled, and, in particular, the speed of increasing of mesh cells height from the wall to the core of the fluid domain. This parameter should

be 1.2, i.e. the cells' growth in height should be with 20% in respect to the previous one, located closer to the blade wall. Likewise is formed also the mesh close to the wall in the hub and close to the wall in the shroud of the fluid domain.

## 2.5 Boundary conditions setup

The timestep parameter by recommendation should be within the region  $0.1/\omega$  to  $1/\omega$ . CFD boundary conditions are as follows: Inlet-Uniform flow  $0.5 \div 25\text{m/s}$ ; Outlet-Reference pressure- $0\text{Pa}$ ; Blade-No slip wall; Hub and Shroud walls-No slip wall. All of them are applied on walls of fluid domain geometry model (fig.4). Definition of fluid includes two fluids air and fresh water. These are two different cases with different materials with different physical properties. During the boundary conditions setup procedure, user must fill box with angular velocity value. In this project is used parameter definition due to full automatize of calculation process and data handling in CFD-Post.

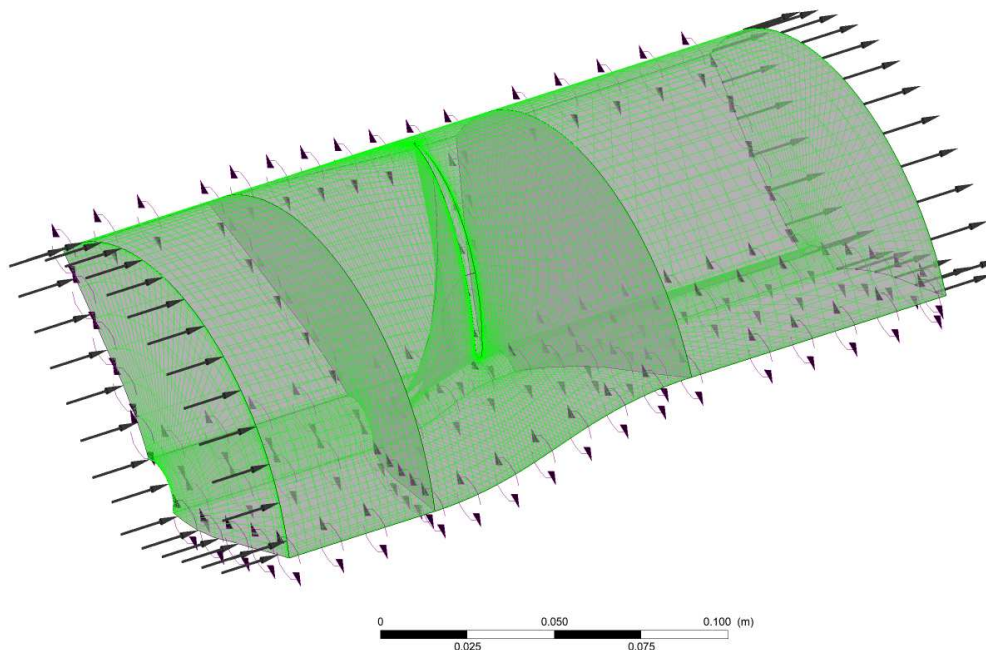


**Fig. 4.** Boundary conditions setup in CFX-Pre

## 2.6 Calculation process

A work station with two CPUs is used in the calculation of the task, where the time for calculating is in the tune of minutes. Furthermore, in view of facilitating the research and the obtaining of the turbine characteristics, the module Design of Experiment of the ANSYS Workbench platform is applied when performing multivariate calculations. Parameters are set in order to start the automated calculation- $U_\infty$ ,  $n$ ,  $T$ ,  $\rho$  and then the borders for changing those parameters are stated. Calculation is completed when reaching a certain target value of the residual Root Mean Square (RMS) 0.0001 with convergence of the calculation process (fig.5,a).

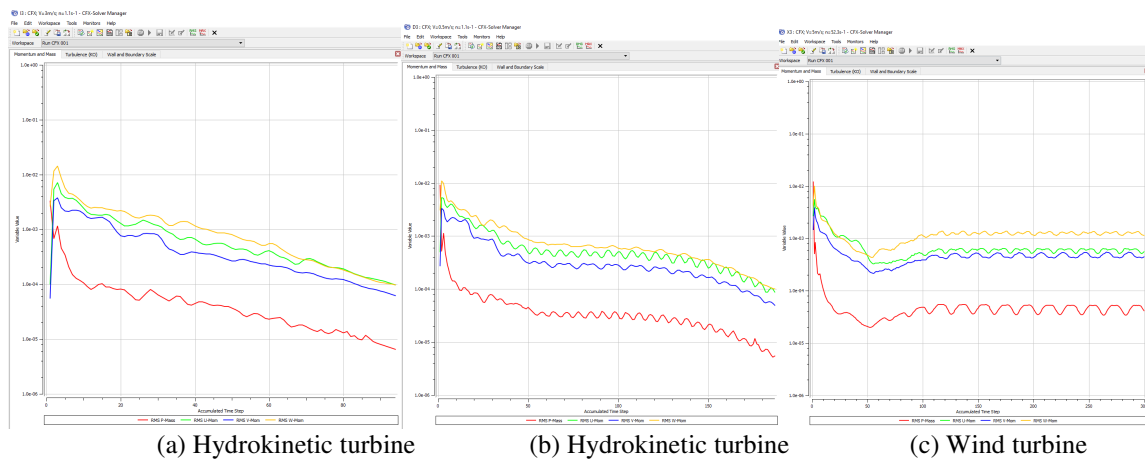


**Fig. 5.** Convergence observation during calculation process

It turns out that in 8% of the simulations there is no convergence of the calculation process observed (fig.5,c). One possible reason for that is the appearance of an unsteady process in the fluid domain. An evidence for that are the pulsations observed in the momentum equation and in the continuity equation on fig.5,b. Oscillations are generated due to the existence of vortices, which break down to smaller ones or the merge of smaller vortices with larger ones. Certainly, the data from those simulations without convergence (fig.5,c) is not reliable, and therefore, it is not taken into consideration with the analysis presented below. URANS, DNS LES modeling should be applied for the calculation of those simulations, while taking into account the unsteady effects. This, however, is substantially impeded due to the shortage of available calculation resources. The above mentioned numerical models are calculated more slowly compared to the RANS models used in the current paper.

## 2.7 Automatically performance calculation of turbine and CFD data handling

For the power calculation it is necessary to derive data about the fluid density (air or water), whereupon the inlet density is averaged for the fluid set temperature. The dependencies are recorded pursuant to the rules of the Command Language. Special attention should be paid on determining the dimensions of the set physical values. The data is derived from the CFD-Post module and is then automatically transferred for analysis to the Design of Experiment module.

## 3 Result and discussion

### 3.1 Performance of wind turbine

We can observe the highly turbulent flow conditions on the downstream side of a turbine, which are caused by its rotation. On fig.6 are surface streamlines on meridional plane for two regimes: 1.  $U_{\infty}=25\text{m/s}$ ;  $n=45\text{rev/s}$  and 2.  $U_{\infty}=5\text{m/s}$ ;  $n=20.9\text{rev/s}$ . The calculated power coefficient with equation (9) for those two regimes is as follows: for first regime  $C_p=0.175$  (fig.6,b), and for second regime  $C_p=0.34$  (fig.6,c).

Fig.6,a presents the air turbine with generated plane, which is well known in studying turbomachinery. It is called meridional plane (the mesh with square cells on fig.6). The velocities  $C_r$  and  $C_z$  are projected in it. The latter velocity is accomplished in a specialized CFX module, called Turbo-Post, and it is well known from the previous versions of the module. The two components of the velocity are used for the calculation of the meridional velocity  $C_m$ . It allows to define surface streamlines on meridional plane at fixed angle  $\theta=30\text{deg}$  in cylindrical coordinates with velocities  $C_r$ ,  $C_z$  and  $C_m$  according software guide (ANSYS CFD-Post User's Guide, 2017). The application of those commands provides the visualization of the flow on fig.6,b and fig.6,c. After the turbine blades, there is a notable intensive vorticity, where one reason for that is the deformation of the outlet velocity triangle. Another reason is the larger pitch between airfoils at shroud and the appearance of substantial radial components of the velocity  $C_m$ . That leads to a distortion of the flow in the impeller. This could be eliminated by optimizing

the blade twisting law by height and modeling a complex 3D shape, namely, blade leaning in circumferential direction (Circumferential Leaning) (Haller B, 1997) and/or axial lean (Sweep) (Japikse D, 1997), (Moustapha H, 2003). The complex 3D shape largely complicates the manufacturing of the impeller when applying conventional production methods, however, it is not that complicated if the 3D Printing technology is used.

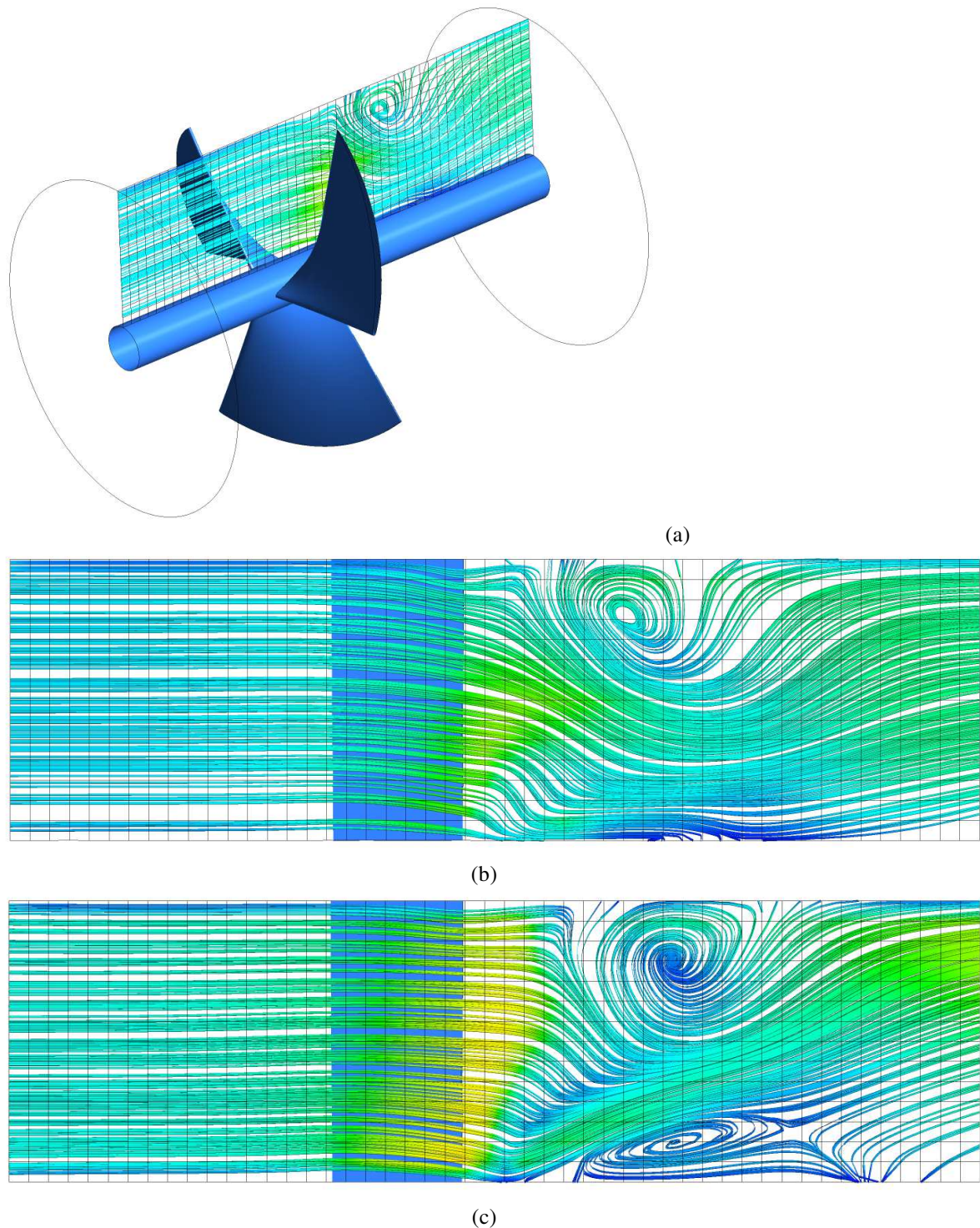


**Fig. 6.** 3D view of the wind turbine (a) and surface streamlines projected on meridional plane for two regimes (b)  $U_\infty=25\text{m/s}$ ;  $n=45\text{rev/s}$ ;  $P_{\text{turb}}=28.6\text{W}$  and (c)  $U_\infty=5\text{m/s}$ ;  $n=20.9\text{rev/s}$ ;  $P_{\text{turb}}=0.45\text{W}$

An outlet guide vane can be used for eliminating the circumferential components after the impeller. It is applied in axial and mixed flow pumps (Japikse D, 1997), however in such additional element there will be friction losses in the blades and secondary vortices at hub and at shroud.

With a lower wind velocity and lower number of revolutions (fig.6,c), there is an evident vortex formed close to the hub after the impeller. This is a result of the low kinetic energy of the incoming inside turbine impeller, and after going out of the turbine blades, the speed  $C_m$  decreases almost twice.

If summarized, the main reasons for the appearance of vortices in the blade-to-blade channel of the wind turbine are:

- a very large pitch between the blades, where the flow passes between them. In order to avoid that, the pitch should be decreased, respectively, the number of blades should be increased.

- the large vortex (fig.6,b and c) close to the shroud after the turbine blades appears due to the separation of the air from the suction side of blade. That vortex is generated at around 20% from the chord, after the leading edge at the suction side of blade.

- the second vortex (fig.6,c) in the area of the hub after the blade appears due to the low velocity of the air after the impeller. The low kinetic energy cannot stabilize the flow and its movement along screw surface.

### 3.2 Performance of hydrokinetic turbine

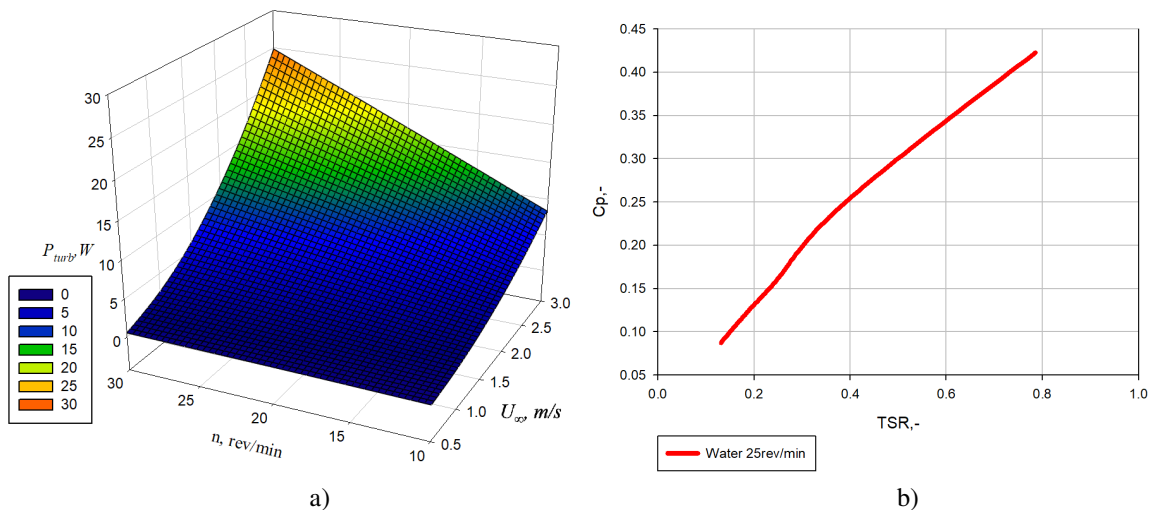


**Fig. 7.** Three dimensional presentation of connection between number of revolutions, inlet water velocity and power of water hydrokinetic turbine (a) and power coefficient variation with TSR (b)

With the calculation with water fluid, the power of the hydrokinetic turbine is higher than when it is working with air. The reason for that is that water density is more than 900 times higher than air density.

Fig.7,a has a similar nature of power  $P_{turb}$  changing depending on the water velocity, compared to studying SEALily water turbine, offered by the company Seaformatics (seaformatics, 2018).

Fig.7,b presents the change of the power coefficient in respect to the TSR. It is evident from the same figure that the maximum speed (Betz limit) of  $C_{pmax}=0.59$  is not reached. The current project does not examine working regimes, where the number of revolutions is high, since power of up to 30W should be reached. The paper examines the power range realized by Waterlily (waterlilyturbine, 2018).

Fig.7,b With the water turbine streaming, it turns out that part of the flow passes between the blades without rendering its kinetic energy to the blades. This is observed with the TSR low values. With those working regimes the turbine, the flow is separated from the blade and vortices are formed. This can be changed if a larger number of blades is chosen, for example 4 or 5. However, objects floating in the water cannot pass through with a large number of blades. The picture changes by increasing the number of revolutions of the impeller, respectively, by increasing TSR. In this case, energy is transferred to the three blades. If the blades' number is larger, there will be a threat of increasing the force of resistance acting on the structure. With water fluid, the density is  $1000 \text{ kg/m}^3$ , and this requires the oversizing of

water turbine's supporting structure. One example may be the water turbine of "Openhydro", which has a low number of revolutions and relatively large number of blades – 10 pcs.

No unscrewing with a high number of revolutions should be allowed with the water turbines because of the threat of cavitation occurring in the tip sections of the blade. Those are the tip sections of the blades with the highest peripheral velocity  $u$ .

#### 4 Conclusions

The purpose of the project is to examine a testing prototype in a wind tunnel. There is not enough detailed information about the geometrical shape of Waterlily turbine's blade, however, using the classical laws for water turbine profiling, known from the specialized literature (Moustapha H, 2003), (Japikse D, 1997) a twisted blade is successfully designed, which is studied under this project.

The research of the wind and water turbine structures has confirmed the conclusion presented by formula (7), namely, that with such relatively small diameter (resp. small area  $A$ ) of the impeller no high power can be expected, yet it is sufficient for the power supply of batteries for lighting, as well as for electronic components in areas, which are far away from the electricity transmission grid. Simulation results gathered with this procedure were well aligned to experimental results from the literature (Mannwell J, 2009).

The purpose of the project is not to increase the power of a small size turbine, but to study a model, which would provide a basis for comparison and a possibility for testing in a wind tunnel at the Technical University – Varna. The next step shall be building a real-life object with a diameter  $D=1\text{m}$  and verification of the obtained results with well-known procedures described in (Japikse D, 1986).

**Acknowledgements** The work described in this paper is the result of a study carried out in project NP12/2018 "Study of three-dimensional turbulent flow passing through hydrokinetic and wind turbines" funded by the State Budget.

#### References

- Moustapha H., M. Zelesky, N. Baines, D. Japikse (2003). Axial and radial turbines. Coincepts NREC
- Japikse D. (1986). Advanced experimental techniques in turbomachinery. Coincepts NREC
- Japikse D., N. Baines (1997). Introduction to turbomachinery. Coincepts ETI and Oxford University Press
- Haller B (1997). Full 3D turbine blade design. VKI Lecture series on secondary and tip clearance flows in axial turbines
- Peake S. (2017). Renewable energy: Power for a sustainable future, 4th edition. Oxford university press
- Miller H. (1974) The STRAFLO turbine: The realisation of Harza's idea. Escher Wyss
- Sheard G. (2014) Stall detection and control in industrial fans. Sigel press
- Djebbari, S., Charpentier, J. F., Scuiller, F., & Benbouzid, M. (2016). Design and performance analysis of double stator axial flux PM generator for rim driven marine current turbines. IEEE Journal of Oceanic Engineering, 41(1), 50-66. <https://doi.org/10.1109/JOE.2015.2407691>

ANSYS CFX-Solver Theory Guide. Release 18.1. (April 2017)

ANSYS CFD-Post User`s Guide. Release 18.0. (January 2017)

Menter F. (2003). Turbulenzmodellierung für Aerodynamische Anwendungen. Aerodynamik und Turbulenzmodellierung. Turbulenzmodelle in der Praxis.

Mannwell J.F, Mcgowan J.G, A.L. Rogers (2009). Wind energy explained: Theory, design and application. 2nd edition.

Fleisinger M., M. Vesenjак (2014). Flow driven analysis of a Darrieus water turbine, Strojniški vesnik - Journal of Mechanical Engineering 60 12, 769-776, <https://doi.org/10.5545/sv-jme.2014.1712>

### Online sources

<https://seaformatics.ca/>, Link visited (September 2018)

<https://waterlilyturbine.com/products/waterlily-turbine>, Link visited (September 2018)

<http://www.greenforwardnews.com/handheld-turbine-can-generate-power-from-wind-or-water/>, Link visited (September 2018)